Supporting Information

Reconfiguration of a mixed-valence copper complex during CO_2 electroreduction promotes CO_2-to-C_2H_4 conversion

Xinkai Wang,‡[a] Yang Yang,‡[a,b] Xian-Ming Zhang*[a,c]

[a]*Key Laboratory of Interface Science and Engineering in Advanced Material (Ministry of Education), College of Chemistry & Chemical Engineering, Taiyuan University of Technology, Taiyuan, 030024, P. R. China.*

[b]*College of Materials Science and Engineering, Qiqihar University, Qiqihar, Heilongjiang, 161006, P. R. China.*

[c]*Key Laboratory of Magnetic Molecules and Magnetic Information Materials (Ministry of Education), Institute of Chemistry and Culture, School of Chemistry & Materials Science, Shanxi Normal University, Taiyuan, 030006, P. R. China.*

‡These authors contributed equally to this work.

E-email: zhangxianming@tyut.edu.cn

Materials

$CuCl_2 \cdot 2H_2O$ (Macklin, 99.99%), 1,10-phenanthroline (Macklin, 97%), 2,2′ -diphenic acid (Macklin, 98%), ethanol (AR) were used without any further purification. The deionized water (18.25 MΩ cm^{-1}) used in all experiments was prepared by ultra-pure purification system (Ulupure).

Synthesis of $[CuCl(phen)_2][CuCl_2]$

Typically, 15 mL of ethanol and 5 mL of deionized water were added into a 50 mL glass beaker and stirred at 500 rpm at room temperature. 0.117 g of 1,10-phenanthroline (phen) and 0.121 g of 2,2' -diphenic acid were sequentially added to the beaker and dissolved gradually. The mixture was stirred for 20 min. Then, 0.085 g of $CuCl_2 \cdot 2H_2O$ was added to the beaker. After the solution was continuously stirred for 1 h, the resulting mixture was transferred into a 50 mL Teflon-lined autoclave and heated at 160 °C for 5 days. After the reaction, dark green crystals were observed on the bottom and wall of the reaction kettle. The remaining solid was collected through continuous centrifugation and washed with water and ethanol until the washing solution was clear. Finally, the solid was dried in a vacuum oven at 60 °C for 12 h to obtain the $[CuCl(phen)_2][CuCl_2]$ catalyst.

Synthesis of $CuCl(phen)_2$

To synthesis $CuCl(phen)_2$, 85 mg $CuCl_2 \cdot 2H_2O$ and 180 mg phen were dissolved in 30 mL methanol and 70 mL CH_2Cl_2 under stirring, respectively. Then, the two solutions

were mixed and heat-treated at 60 ℃ for 12 h. After the reaction, the solvent was removed by rotary evaporation. The remaining green powder was washed with water and CH_2Cl_2 until the washing solution was clear. Finally, the solid powder was dried in a vacuum oven at 60 °C for 12 h to obtain the $CuCl(phen)_2$ catalyst.

Characterizations

X-ray diffiraction (XRD) patterns were collected on a Smartlab X-ray diffractometer (Rigaku, Japan). Scanning electron microscopy (SEM) images were obtained using a JSM-7900F field emission scanning electron microscope (JEOL, Japan). Transmission electron microscopy (TEM) images were acquired on a F200 transmission electron microscope (JEOL, Japan). X-ray photoelectron spectroscopy (XPS) measurements were performed on an ESCALAB Xi+ X-ray photoelectron spectrometer (Thermo Scientific, USA). In situ attenuated total reflection infrared (ATR-IR) experiments were performed on an Invenion S spectrometer (Bruker, Germany).

Preparation of working electrodes

The catalyst ink was prepared by ultrasonically dispersing 5 mg catalyst in a mixture of 600 μL isopropyl alcohol, 350 μL of deionized water and 50 μL of 5 wt% Nafion solution. After sonication for 1 h, 10 μL of the ink was dripped on glassy carbon electrode with a 5 mm diameter. Alternatively, 200 μL of the ink was coated on the carbon paper with an exposed area of 1×1 cm^2. Finally, these prepared electrodes were dried at room temperature for 3 h to obtain working electrodes.

Electrochemical CO_2 reduction testing in an H-type cell

ECO_2RR tests were performed in a three-electrode two-compartment H-cell (CH2010-S, ida) controlled by an electrochemical workstation (CHI760e, Chenhua). The two chambers were separated by a proton exchange membrane (Nafion N117, Dupont). The working electrode was a glassy carbon electrode coated with catalyst, the reference electrode was an Ag/AgCl electrode (saturated KCl solution), and the counter electrode was a platinum sheet electrode. The working electrode and reference electrode were placed in the cathodic cell, while the counter electrode was placed in the anodic cell. Each cell was filled with 30 mL of 0.1 M $KHCO_3$ solution. During the ECO_2RR experiments, the flow rate of CO_2 was maintained at 25 mL min^{-1}, and the cathode chamber was stirred at 500 rpm throughout the test. Before the test, CO_2 gas was pumped into the cathode chamber electrolyte for 30 min, discharging the soluble oxygen in the solution to obtain a CO_2-saturated electrolyte. All test potentials without iR compensation were converted to RHE by measuring the Ag/AgCl electrode using the Nernst formula：

$$E \text{ (vs. RHE)} = E \text{ (vs. Ag/AgCl)} + 0.197 \text{ V} + 0.059 \times pH$$

Product analysis

An Agilent 8890 gas chromatograph (GC) was applied to quantitative analysis of gaseous products. And liquid products were characterized by a Bruker AVANCE NEO 600 ^1H nuclear magnetic resonance (NMR) spectrometer. In this experiment, 500 μL electrolyte was mixed with 100 μL D_2O solution and 100 μL 10 mmol L^{-1} dimethyl

sulfoxide (DMSO) solution, and DMSO was used as the internal standard solution.

The Faraday efficiency (FE) of the product was calculated based on the gas chromatographic peak area, and the formula was as follows[1]:

$$FE_{gas} = \frac{\alpha \times n \times F}{Q} = \frac{\alpha \times F \times p \times V \times 10^{-6}\,(m^3\,mL^{-1}) \times v(vol\%)}{R \times 298.15\,(K) \times I(C\,s^{-1}) \times 60\,(s\,min^{-1})} \times 100\%$$

In this equation, α represents the number of electrons transferred by a particular product, Q represents the total charge generated throughout the electrolysis process, p represents the atmospheric pressure (101.325 kPa), V represents the gas flow rate, v (vol%) is the concentration of the gas measured by the GC, R represents the ideal gas constant (R = 8.314 J (mol·K)$^{-1}$) and F represents Faraday's constant (F = 96485 C mol^{-1}).

The FE of liquid products was calculated as follows as previous report[2]:

$$FE_{liquid} = \frac{C_{product} \times V \times \alpha \times F}{Q} \times 100\%$$

Where $C_{product}$ is the concentration of the liquid product, V is the volume of the electrolyte and Q is the total charge of the CO_2 electroreduction.

In situ ATR-IR measurements details

Experimental conditions of ATR-IR internal reflection mode: 15 μL of the catalyst ink was dripped to the center of the gold-coated silicon crystal and dried for 2 h at room temperature. The silicon crystal, loaded with catalyst, was mounted in a three-electrode system within an in-situ infrared reaction cell. The silicon crystal was connected to a conductive copper foil, which served as the working electrode. In addition, an Ag/AgCl

electrode was used as the reference electrode, and the platinum wire was used as the counter electrode to form a three-electrode system. 0.1 M $KHCO_3$ solution was added into the reaction cell. The reaction cell was purified with high-purity CO_2 gas for 30 min before the experiment, and CO_2 gas was continuously passed through the cell during the experiment at a flow rate of 25 mL min^{-1}. The cell was connected to an electrochemical workstation (CHI760e, Chenhua) for an i-t testing within the range of -1.3 to -0.2 V vs. RHE. Spectra was recorded at open circuit voltage (OCP) for comparison.

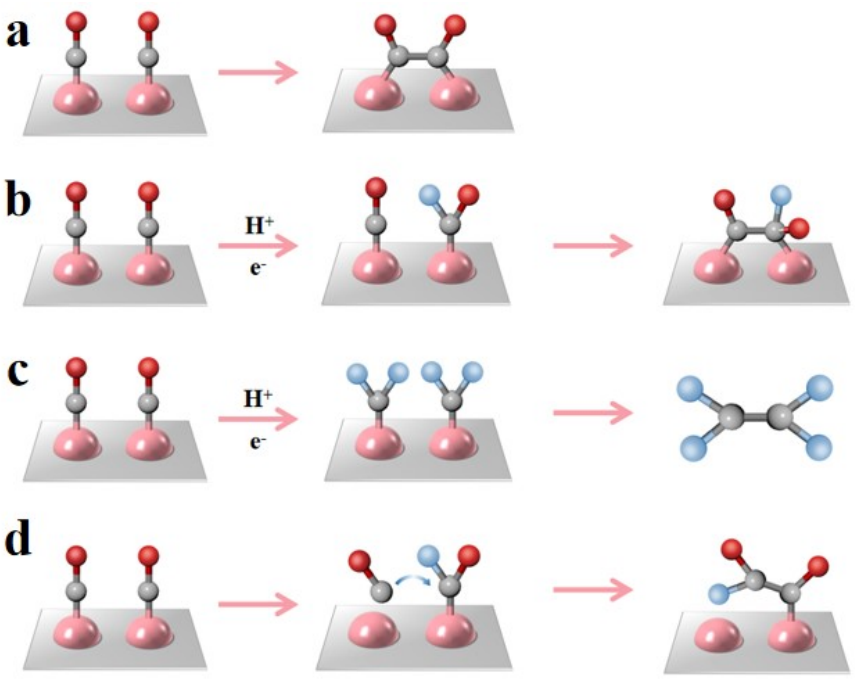

Figure S1. Possible C-C coupling mechanisms in ECO_2RR process. (a, b) Dimerization mechanism. (c) Carbene mechanism. (d) "Insertion of CO in *CHO" mechanism. Noted: Cu, Pink; C, Gray; O, Red; H, Blue.

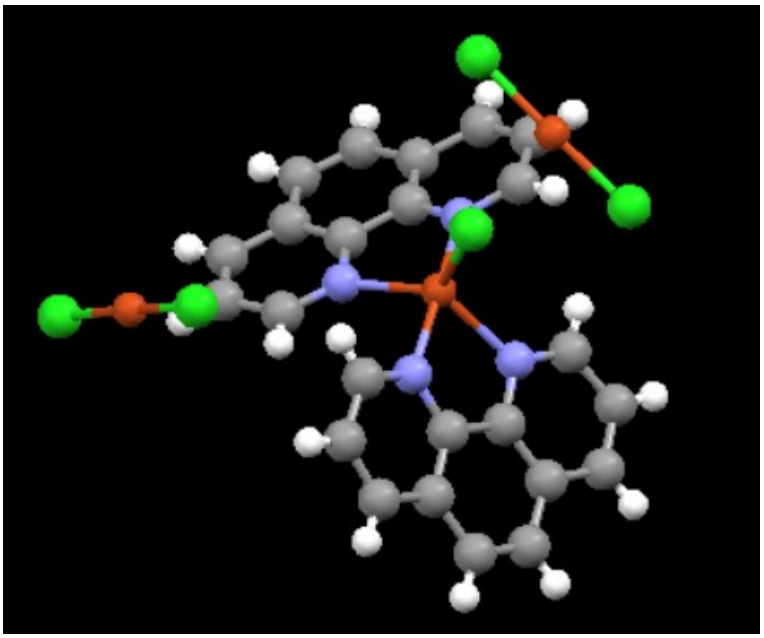

Figure S2. Structure of $[CuCl(phen)_2][CuCl_2]$. Noted: Cu, Orange; Cl, Green; N, Blue; C, Gray; H, White. The $[CuCl(phen)_2]^+$ cation contains a five-coordinated Cu(II) ion, which coordinates with one Cl atom and four N atoms from two phenanthroline (phen) ligands, forming a triangular bipyramidal structure.

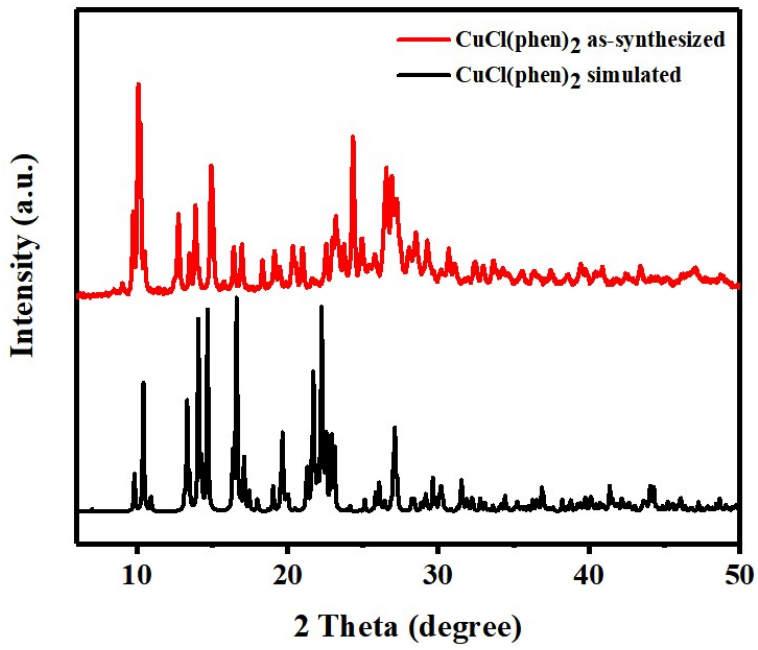

Figure S3. Simulated and as-synthesized XRD patterns of $CuCl(phen)_2$.

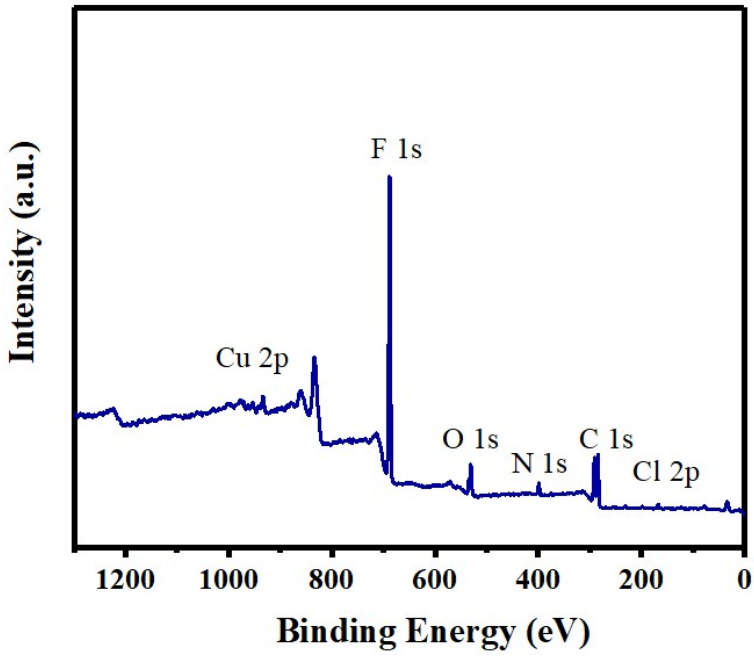

Figure S4. XPS survey spectrum of $[CuCl(phen)_2][CuCl_2]$. The O and F elements in the XPS spectrum are derived from the Nafion solution.

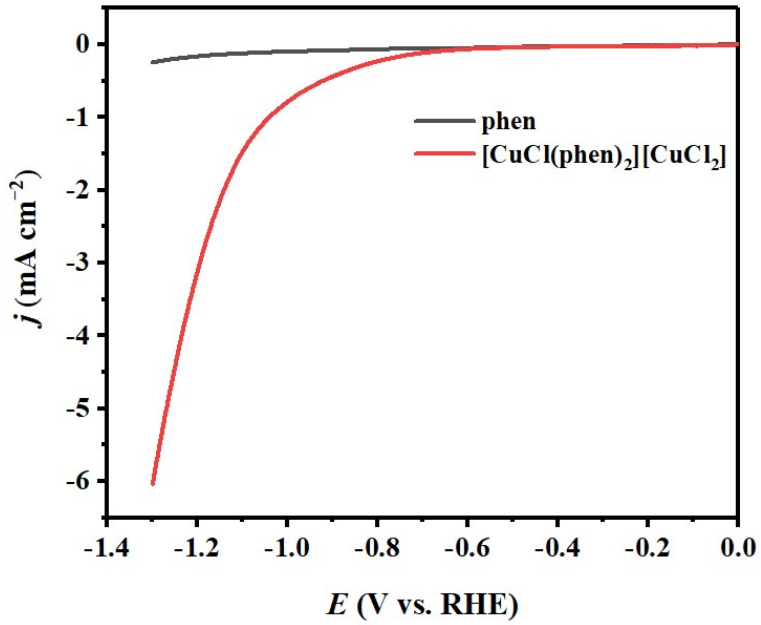

Figure S5. LSV curves of phen and $[CuCl(phen)_2][CuCl_2]$ in CO_2-saturated 0.1 M $KHCO_3$ solution.

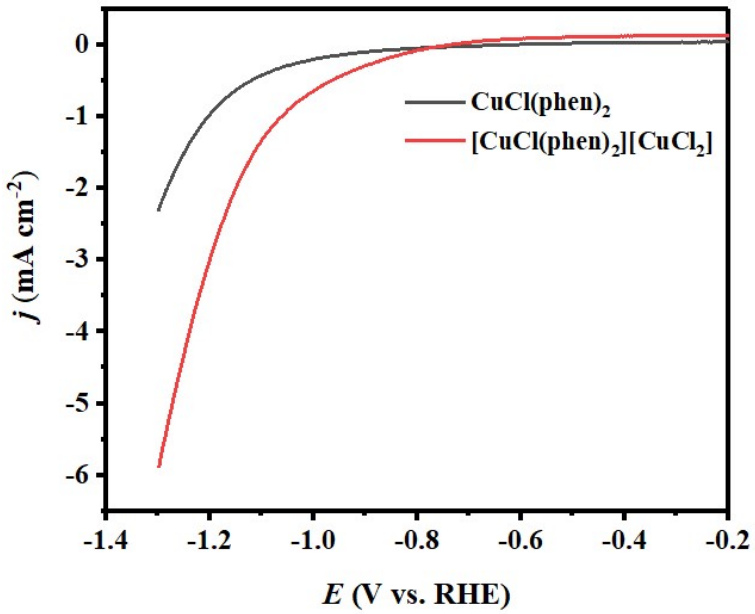

Figure S6. LSV curves of $[CuCl(phen)_2][CuCl_2]$ and $CuCl(phen)_2$ in CO_2-saturated 0.1 M $KHCO_3$ solution.

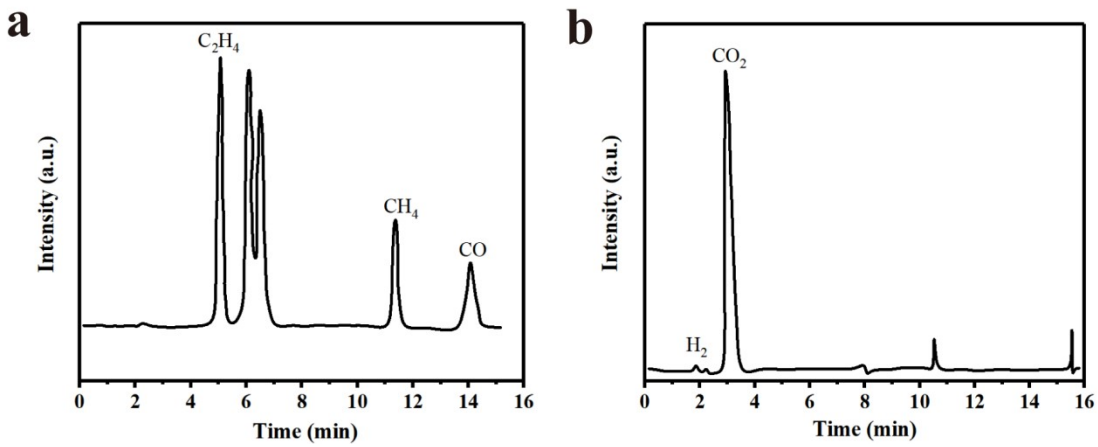

Figure S7. GC profiles of the standard gases with different concentrations. GC spectra peaks of (a) C_2H_4, CH_4 and CO, (b) H_2 and CO_2. The concentrations of C_2H_4, CH_4, CO and H_2 are 222.4, 224.1, 221.6 and 502.4 ppm, respectively.

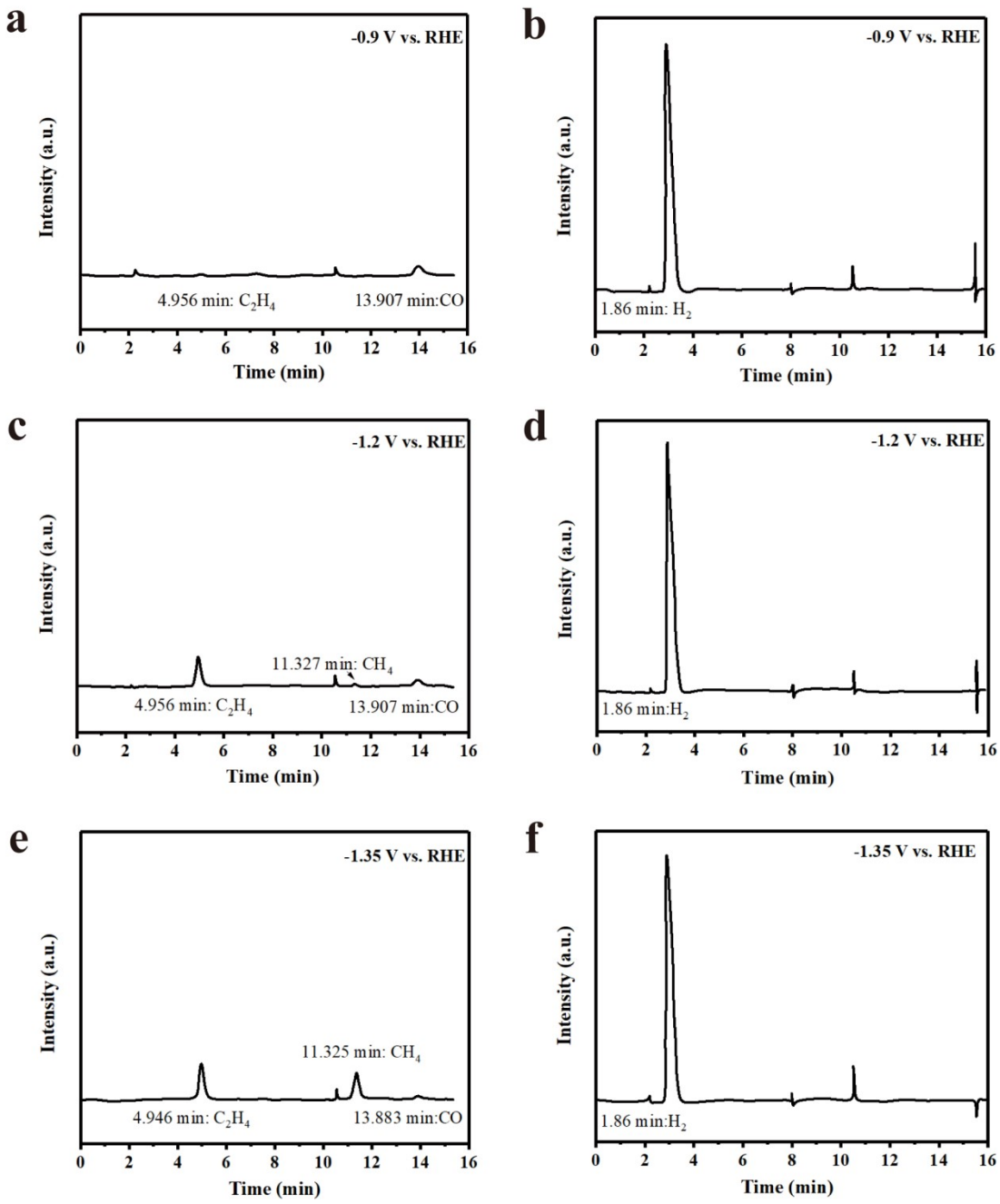

Figure S8. GC profiles of $[CuCl(phen)_2][CuCl_2]$ catalyzing ECO_2RR with different potentials: (a, b) -0.9 V vs. RHE, (c, d) -1.2 V vs. RHE and (e, f) -1.35 V vs. RHE.

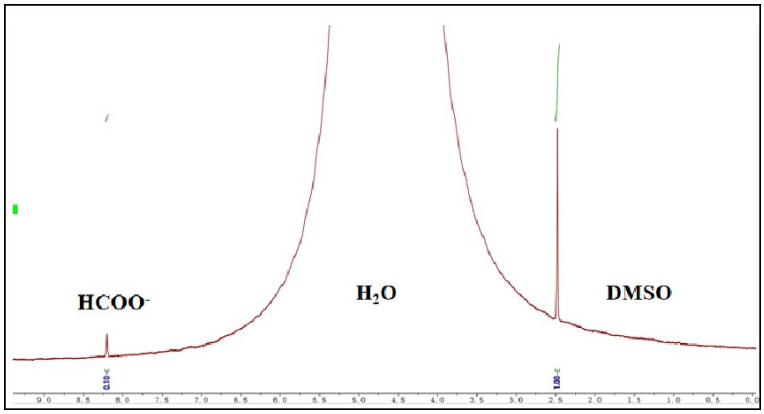

Figure S9. ^{1}H NMR spectrum of the liquid product catalyzed by $[CuCl(phen)_2][CuCl_2]$ at -1.2 V vs. RHE after the ECO_2RR test. The concentration of liquid product was measured using an internal standard, DMSO.

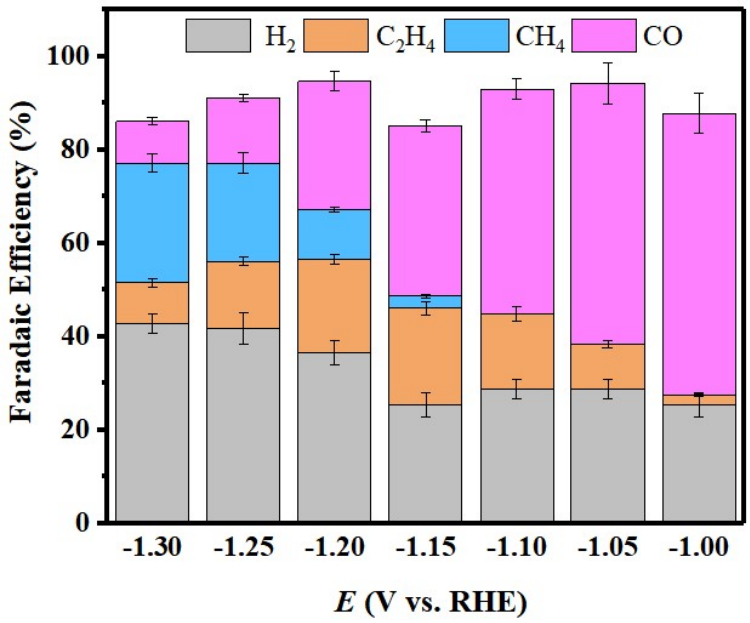

Figure S10. FEs of different reduced gasous products on $CuCl(phen)_2$ catalyst at different potentials.

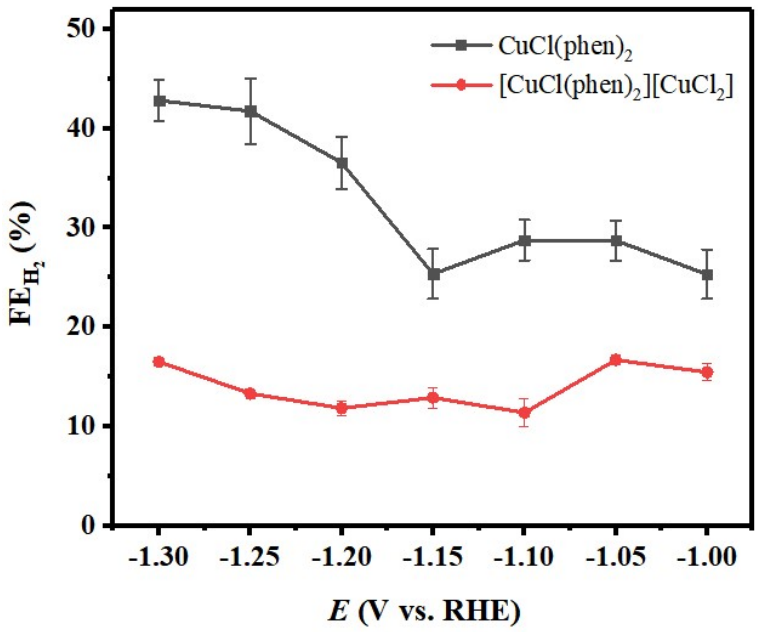

Figure S11. FE_{H2} of $[CuCl(phen)_2][CuCl_2]$ and $CuCl(phen)_2$ at different potentials.

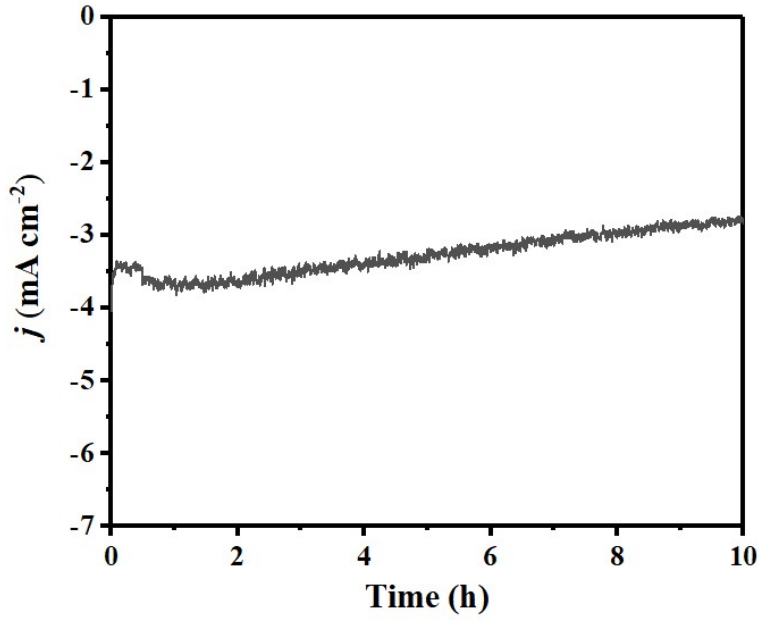

Figure S12. Continuous i-t curve of $[CuCl(phen)_2][CuCl_2]$ at -1.2 V vs. RHE.

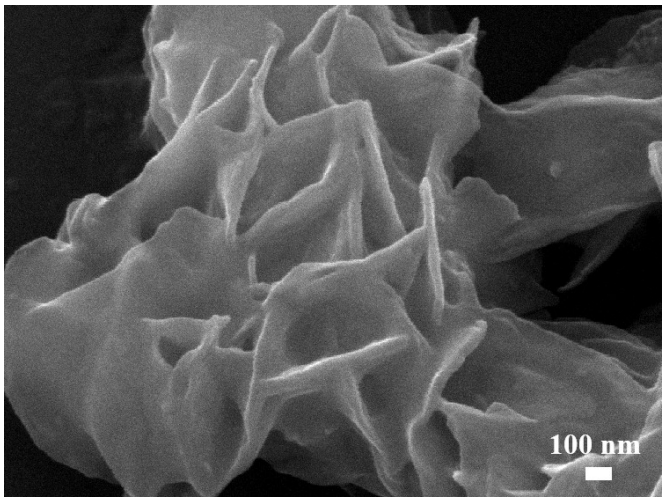

Figure S13. SEM image of $[CuCl(phen)_2][CuCl_2]$ after the ECO_2RR.

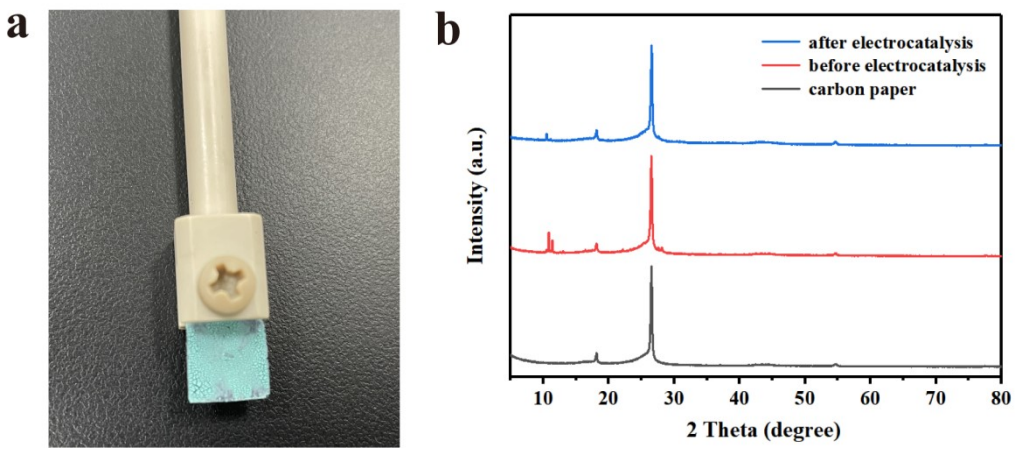

Figure S14. (a) Photograph of $[CuCl(phen)_2][CuCl_2]$ dripping on carbon paper. (b) XRD patterns of $[CuCl(phen)_2][CuCl_2]$ dripping on carbon paper before and after the ECO_2RR tests and blank carbon paper.

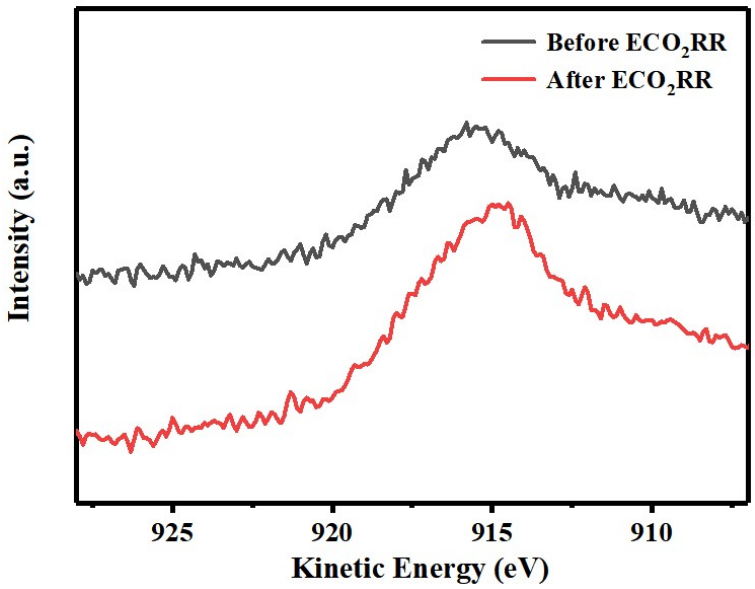

Figure S15. Cu Auger spectrum of $[CuCl(phen)_2][CuCl_2]$ before and after the ECO_2RR test at -1.2 V vs. RHE. The shift of Cu Auger peak towards lower kinetic energy after ECO_2RR, which indicates an increase in electron cloud density, signifying the reduction from Cu(II) to Cu(I). Meanwhile, the narrowing of Auger peak width implies more homogeneous chemical state of Cu species after the ECO_2RR test[3].

Table S1. Summary of the ECO_2RR performances for different Cu-based complexes and Cu metal-organic frameworks (MOFs). All studies were carried out in H-type cells with aqueous electrolyte systems.

Catalysts	Electrolyte	*E* (V vs. RHE)	C_2H_4 (FE, %)	Ref.
$[CuCl(phen)_2][CuCl_2]$	**0.1M $KHCO_3$**	**-1.2**	**47**	**This work**
$CuCl(phen)_2$	0.1M $KHCO_3$	-1.0	2	4
CuPPh	0.1M $KHCO_3$	-0.96	45	5
$[Cu_2(phen)_2(OH)_2(H_2O)_2]$ $[Cu_2(phen)_2(OH)_2Cl_2]Cl_2 \cdot 6H_2O$	0.1M $CsHCO_3$	-1.25	42	6
$[Cu_2(NTB)_2Cl_2]^{2+}$	0.1M KCl	-1.28	42	7
PcCu-Cu-O	0.1M $KHCO_3$	-1.2	50	8
BIF-102NSs	0.5M $KHCO_3$	-1.0	11	9
CuTAPP	0.5M $KHCO_3$	-1.0	3	10
Cu_2BDC	0.1M KI	-1.3	34	11
Au NN@PCN-222(Cu)	0.1M $KHCO_3$	-1.2	53	12
S-HKUST-1	0.1M $KHCO_3$	-1.3	60	13

References

1 Yang HB, Hung SF, Liu S, Yuan K, Miao S, Zhang L, Huang X, Wang HY, Cai W, Chen R, Gao J. Atomically dispersed Ni (i) as the active site for electrochemical CO_2 reduction. *Nat. Energy*. 2018, **3 (2)**, 140-147.

2 Liu S, Wang T, Liu X, Liu J, Shi H, Lai J, Liang J, Li S, Cai Z, Huang Y, Li Q. In Situ Dissociated Chalcogenide Anions Regulate the Bi-Catalyst/Electrolyte Interface with Accelerated Surface Reconstruction toward Efficient CO_2 Reduction. *ACS Catal*. 2023, **14 (1)**, 489-497.

3 Zhang W, Huang C, Xiao Q, Yu L, Shuai L, An P, Zhang J, Qiu M, Ren Z, Yu Y. Atypical Oxygen-Bearing Copper Boosts Ethylene Selectivity toward Electrocatalytic CO_2 Reduction. *J. Am. Chem. Soc.* 2020, **142 (26)**, 11417-11427.

4 Wang J, Gan L, Zhang Q, Reddu V, Peng Y, Liu Z, Xia X, Wang C, Wang X. A water-soluble Cu complex as molecular catalyst for electrocatalytic CO_2 reduction on graphene-based electrodes. *Adv. Energy Mater*. 2019, **9**, 1803151.

5 Wang P, Li T, Wu Q, Du R, Zhang Q, Huang WH, Chen CL, Fan Y, Chen H, Jia Y, Dai S. Molecular assembled electrocatalyst for highly selective CO_2 fixation to C_{2+} products. *ACS Nano*. 2022, **16**, 17021-17032.

6 Liu N, Bartling S, Springer A, Kubis C, Bokareva OS, Salaya E, Sun J, Zhang Z, Wohlrab S, Abdel-Mageed AM, Liang HQ. Heterogenized Molecular Electrocatalyst Based on a Hydroxo-Bridged Binuclear Copper (II) Phenanthroline Compound for Selective Reduction of CO_2 to Ethylene. *Adv. Mater*. 2024, **36**, 2309526.

7 Balamurugan M, Jeong HY, Choutipalli VS, Hong JS, Seo H, Saravanan N, Jang JH, Lee KG, Lee YH, Im SW, Subramanian V. Electrocatalytic reduction of CO_2 to ethylene by molecular Cu-

complex immobilized on graphitized mesoporous carbon. *Small*. 2020, **16**, 2000955.

8 Qiu XF, Zhu HL, Huang JR, Liao PQ, Chen XM. Highly selective CO_2 electroreduction to C_2H_4 using a metal-organic framework with dual active sites. *J. Am. Chem. Soc*. 2021, **143**, 7242-7246.

9 Shao P, Zhou W, Hong QL, Yi L, Zheng L, Wang W, Zhang HX, Zhang H, Zhang J. Synthesis of a boron-imidazolate framework nanosheet with dimer copper units for CO_2 electroreduction to ethylene. *Angew. Chem. Int. Ed*. 2021, **60**, 16687-16692.

10 Yu P, Lv X, Wang Q, Huang H, Weng W, Peng C, Zhang L, Zheng G. Promoting electrocatalytic CO_2 reduction to CH_4 by copper porphyrin with donor-acceptor structures. *Small*. 2023, **19**, 2205730.

11 Zhou X, Dong J, Zhu Y, Liu L, Jiao Y, Li H, Han Y, Davey K, Xu Q, Zheng Y, Qiao SZ. Molecular scalpel to chemically cleave metal-organic frameworks for induced phase transition. *J. Am. Chem. Soc*. 2021, **143**, 6681-6690.

12 Xie X, Zhang X, Xie M, Xiong L, Sun H, Lu Y, Mu Q, Rummeli MH, Xu J, Li S, Zhong J. Au-activated N motifs in non-coherent cupric porphyrin metal organic frameworks for promoting and stabilizing ethylene production. *Nat. Commun*. 2022, **13**, 63.

13 Wen CF, Zhou M, Liu PF, Liu Y, Wu X, Mao F, Dai S, Xu B, Wang XL, Jiang Z, Hu P. Highly Ethylene-Selective Electrocatalytic CO_2 Reduction Enabled by Isolated Cu-S Motifs in Metal-Organic Framework Based Precatalysts. *Angew. Chem. Int. Ed*. 2022, **61**, 202111700.